ISBN: 978-3-95450-225-7 ISSN: 2673-5571 doi:10.18429/JACoW-HB2021-MOP15

THRESHOLD FOR LOSS OF LONGITUDINAL LANDAU DAMPING IN DOUBLE HARMONIC RF SYSTEMS

L. Intelisano*[1], H. Damerau, I. Karpov, CERN, Geneva, Switzerland
[1]Sapienza Università di Roma, Rome, Italy

Abstract

Landau damping is a natural stabilization mechanism to mitigate coherent beam instabilities in the longitudinal phase space plane. In a single RF system, binominal particle distributions with a constant inductive impedance above transition (or capacitive below) would lead to a vanishing threshold for the loss of Landau damping (LLD), which can be avoided by introducing an upper cutoff frequency to the impedance. This work aims at expanding the recent loss of Landau damping studies to the common case of double harmonic RF systems. Special attention has been paid to the configuration in the SPS with a higher harmonic RF system at four times the fundamental RF frequency, and with both RF systems in counter-phase (bunch shortening mode). Refined analytical estimates for the synchrotron frequency distribution allowed to extend the analytical expression for the loss of Landau damping threshold. The results are compared with semi-analytical calculations using the MELODY code, as well as with macroparticle simulations in BLonD.

INTRODUCTION

Landau damping [1] provides beam stability to a wide variety of working high beam intensity accelerators. In general, loss of Landau damping (LLD) occurs when the frequency of the coherent bunch oscillations moves outside the incoherent band. In the longitudinal plane, this natural stabilization mechanism is achieved by means of the synchrotron frequency spread which is caused by the nonlinearities of the RF fields. Synchrotron frequency spread, can be enhanced by using multiple RF systems. In particular, higher harmonic RF systems are operated in many accelerators either to change the bunch shape (even split it) or to increase the synchrotron frequency spread inside the bunch, as shown in Fig. 1. In this work we focused mainly on the Super Proton Synchrotron (SPS) configuration namely a 4th harmonic RF system (higher harmonic RF system at four times the fundamental RF frequency) and the case above transition energy. For such double harmonic RF systems, the total voltage seen by the particles is defined as:

$$V_{\mathrm{RF}}(\phi) = V_0[\sin(\phi + \phi_{s_0}) + r\sin\left(n\phi + n\phi_{s_0} + \Phi_2\right)], \quad (1)$$

where V_0, r and ϕ_{s0} are respectively the voltage magnitudes of the main harmonic RF system, the voltage ratio between the higher harmonic and the fundamental harmonic RF system, and the phase of the synchronous particle. As far as ϕ, n and Φ_2 are concerned, they represent the phase offset with respect to the synchronous particle, the harmonic number ratio and the relative phase between the two RF systems. Depending on the relative Φ_2, two operating modes are defined; in particular in the case of two RF systems in phase, bunches would get shorter with respect to the single RF system case. This operating mode is called bunch shortening mode (BSM). On the other hand, in the case of both RF systems in counter-phase, one refers to the bunch lengthening operating mode (BLM).

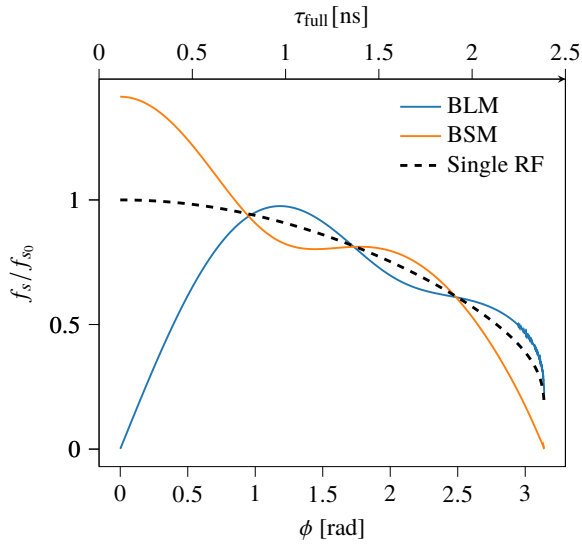

Figure 1: Synchrotron frequency spread normalized to the small-amplitude synchrotron frequency in a single RF system as a function of the maximum phase deviation of the particle. Two different operating modes for the 4th harmonic RF system are plotted, for the BSM (orange) and the BLM (blue) with $r = 0.25$. The curves are compared with the conventional single RF system case (black dashed line). The axis top concerning the full bunch length τ_{full} aims to be a reference for Fig 2.

Recent studies [2] prove that for a single RF system, binomial family of particle distributions with a constant inductive impedance $\mathrm{Im}Z/k$ above transition energy, leads to a vanishing LLD threshold. However, this is avoidable by introducing an upper cutoff frequency f_c to the impedance. In the present work, an analytical expression of the LLD threshold in BSM, above transition energy, will be derived. Furthermore, its results will be compared with semianalytical calculations, using the MELODY code [3], and macroparticle simulations in BLonD [4]. Moreover, we will study the LLD by analyzing the offset evolution of the bunch after a rigid-dipole perturbation.

* leandro.intelisano@cern.ch

Content from this work may be used under the terms of the CC BY 3.0 licence (© 2021). Any distribution of this work must maintain attribution to the author(s), title of the work, publisher, and DOI

ISBN: 978-3-95450-225-7 ISSN: 2673-5571 doi:10.18429/JACoW-HB2021-MOP15

Content from this work may be used under the terms of the CC BY 3.0 licence (© 2021). Any distribution of this work must maintain attribution to the author(s), title of the work, publisher, and DOI

BUNCH SHORTENING MODE ABOVE TRANSITION ENERGY

In this section, we will focus mainly on the LLD in BSM above transition energy. For convenience, the whole analysis is performed with the set of variables $(\mathcal{E}, \psi)$ for the description of the longitudinal beam dynamics, which correspond respectively to the energy and phase of the synchrotron oscillations.

$$\begin{aligned} \mathcal{E} &= \frac{\dot{\phi}^2}{2\omega_{s0}^2} + U_t(\phi) \\ \psi &= \mathrm{sgn}(\eta \Delta E)\frac{\omega_s(\mathcal{E})}{\sqrt{2}\omega_{s0}} \int_{\phi_{\max}}^{\phi} \frac{d\phi'}{\sqrt{\mathcal{E} - U_t\,(\phi')}} \end{aligned}, \tag{2}$$

where ΔE and ω_{s_0} are the energy offset with respect to the synchronous particle and the angular frequency of small amplitude synchrotron oscillations in single RF, $\eta = 1/\gamma_{\mathrm{tr}}^2 - 1/\gamma^2$ is the slip factor, and γ_{tr} is the Lorentz factor at transition energy. In general, the total potential U_t is related to the sum voltage Eq. (1) in the following way:

$$U_t(\phi) = \frac{1}{V_0 \cos\phi_{s0}} \int_{\Delta\phi_s}^{\phi} \left[V_t\,(\phi') - V_0 \sin\phi_{s0}\right] d\phi'. \tag{3}$$

The synchronous phase shift $\Delta\phi_s$ due to intensity effects must satisfy the relation $V_0 \sin(\phi_{s0}) = V_{\mathrm{RF}}(\Delta\phi_s) + V_{\mathrm{ind}}(\Delta\phi_s)$, where $V_{\mathrm{ind}}(\Delta\phi_s)$ is the induced voltage.

This work is mainly based on considering particle distribution of a binomial family

$$g(\mathcal{E}) = \left(1 - \frac{\mathcal{E}}{\mathcal{E}_{\max}}\right)^{\mu}, \tag{4}$$

which, depending on μ, covers most of the realistic bunch distributions in proton synchrotrons.

Analytical Equation of the LLD Threshold

In order to derive an analytical expression of the LLD threshold in BSM for the dipole mode, we will follow a similar procedure as in Ref. [2]. The procedure consists of solving the Lebedev equation [5] in presence of a constant inductive impedance $\mathrm{Im}Z/k$=const. We can define the LLD threshold as the point at which the coherent mode frequency Ω equals the maximum incoherent frequency; in other words $\Omega = \max\left[\omega_s(\mathcal{E})\right]$. The general LLD threshold for a binomial distribution can be derived starting equation [2]:

$$\zeta_{\mathrm{th}} = -h\left[\sum_{k=-\infty}^{\infty} G_{kk}(\Omega)\frac{Z_k(\Omega)/k}{\mathrm{Im}\,Z/k}\right]^{-1}, \tag{5}$$

where $G_{kk}(\Omega)$, h and ζ represent respectively beam transfer matrices [6], the harmonic number and the dimensionless intensity parameter:

$$\zeta \triangleq -\frac{qN_p h^2 \omega_0 Z_{\mathrm{norm}}}{V\cos\phi_{s0}}. \tag{6}$$

The impedance Z_{norm} is an arbitrary normalization factor in units of Ohm.

An analytical expression for the synchrotron frequency spread, as a function of the energy of synchrotron oscillations, can be derived from the oscillation period shown on the right hand side of the second equation (2). Thus, since $\omega_s(\mathcal{E}) = 2\pi/T_s(\mathcal{E})$, for short bunches, we obtain [7]:

$$\frac{\omega_s(\mathcal{E})}{\omega_{s0}} = \sqrt{1+nr}\left(1 - \frac{1+rn^3}{(1+rn)^2}\frac{\mathcal{E}}{8}\right). \tag{7}$$

Therefore, considering the first azimuthal mode (dipole mode; $m = 1$), LLD in BSM occurs when $\Omega = \omega_s(0)$; where for Eq. (7) $\omega_s(0) = \omega_{s0}\sqrt{1+nr}$. Furthermore, considering only the dipole mode, the matrix $G_{kk}(\Omega)$ can be written as:

$$G_{kk}(\Omega) = -i\frac{\omega_{s0}}{\pi A_N}\int_0^{\mathcal{E}_{\max}} \frac{dg(\mathcal{E})}{d\mathcal{E}}\frac{|I_{1k}(\mathcal{E})|^2}{\Omega - \omega_s(\mathcal{E})}d\mathcal{E}, \tag{8}$$

with the normalization factor

$$A_N = \omega_{s0}\int_0^{\mathcal{E}_{\max}} \frac{g(\mathcal{E})}{\omega_s(\mathcal{E})}d\mathcal{E}. \tag{9}$$

As far as the function I_{mk} [5] is concerned, it is expressed as

$$I_{1k}(\mathcal{E}) = \frac{1}{2\pi}\int_{-\pi}^{\pi} e^{i\frac{k}{h}\phi(\mathcal{E},\psi) - i\psi}d\psi. \tag{10}$$

In the case of small amplitude, the integral can be reduced to the Bessel function of the first kind:

$$I_{1k}(\mathcal{E}) \approx iJ_1\left(\frac{k}{h}\sqrt{\frac{2}{1+rn}\mathcal{E}}\right). \tag{11}$$

Equations (8) can be evaluated analytically and used to deduce the threshold Eq. (10) for the BSM case. However, for $\mathrm{Im}Z/k$ = const, it leads to a vanishing threshold $\zeta_{\mathrm{th}} = 0$. Hence, in order to avoid this zero LLD threshold, we considered a finite cutoff frequency f_c to the impedance, obtaining:

$$\zeta_{\mathrm{th}} \approx \frac{1+rn^3}{(1+rn)^{1/2}}\frac{\pi\phi_{\max}^5 h}{32\mu(\mu+1)\chi\left(k_{max}\phi_{max}/h,\mu\right)}; \tag{12}$$

where $\phi_{\max}$ represents the maximum phase deviation or, equivalently, the bunch length in radians (full bunch length $\tau_{\mathrm{full}} = [\phi_{\max}(\mathcal{E}) - \phi_{\min}(\mathcal{E})]/\omega_{\mathrm{RF}}$). The function $\chi\,(y,\mu)$, is related to the generalized hypergeometric function, according to:

$$\chi(y,\mu) = y\left[1 - {}_2F_3\left(\frac{1}{2},\frac{1}{2};\frac{3}{2},2,\mu;-\frac{y^2}{1+rn}\right)\right]. \tag{13}$$

Analysing Eq. (12), we can notice that the LLD threshold depends on the voltage ratio and the order n of the harmonic RF system. In the case of switching off the second RF system ($r = 0$), Eq. (12) simplifies to the LLD threshold for the single RF system case [2]. In Fig. 2 we compared the LLD

ISBN: 978-3-95450-225-7 ISSN: 2673-5571 doi:10.18429/JACoW-HB2021-MOP15

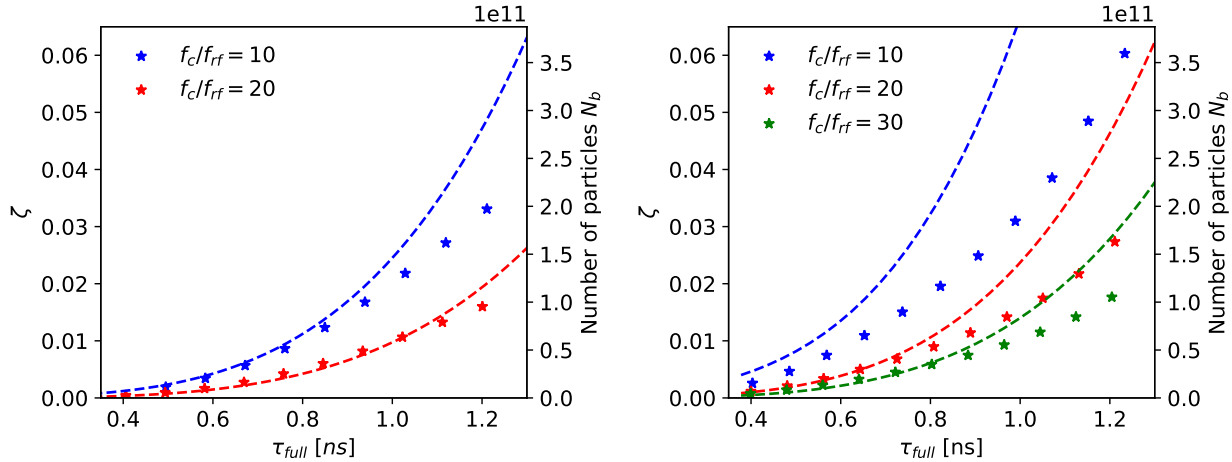

Figure 2: The LLD threshold, for the 2nd (left; $n = 2$) and for the 4th (right; $n = 4$) harmonic RF system case, as a function of the full bunch length. The thresholds, using MELODY for different impedance cutoff frequencies, are calculated. The analytical predictions are shown as dashed lines and computed based on $Z_{\text{norm}} = 0.07$ Ohm, $r = 0.25$ and $\mu = 2$.

thresholds, as a function of the full bunch length, for different cutoff frequencies. On the left figure, we can observe that the 2nd harmonic case (Fig. 2, left) is in good agreement with the exact solution computed with MELODY for the two different cutoff frequencies. On the other hand, the 4th harmonic case (Fig. 2, right) shows that the agreement is less good when decreasing the cutoff frequency. This is due to the fact that the threshold Eq. (12) does not hold for high intensities. Furthermore, we can observe that the LLD threshold depends inversely on the frequency cutoff, which is consistent with the case of the single RF system above transition energy [2].

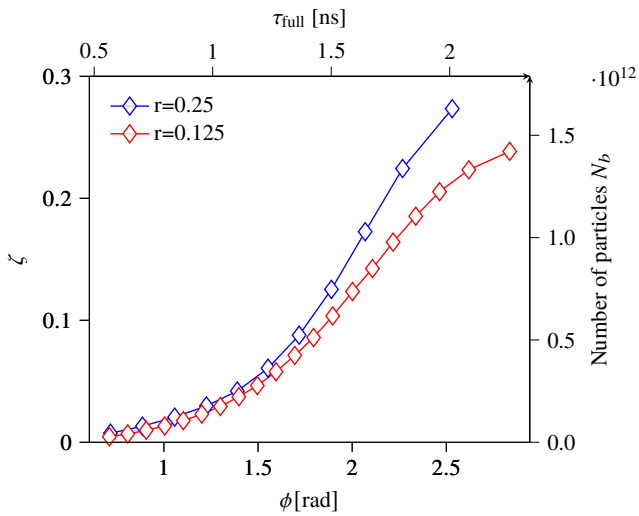

Figure 3: The LLD thershold as a function of the bunch length. The thresholds are computed for the voltage ratio $r = 0.25$ (blue) and $r = 0.125$ (red) by considering $Z_{\text{norm}} = 0.07$ Ohm with a cutoff at $f_c = 4$ GHz and μ=2.

Figure 3 shows that for even longer bunch length, the LLD threshold preserves its monotonic behaviour. This is in contradiction with what has been observed in Ref. [8] which observed a decrease of the LLD threshold along the portion for which the derivative of the frequency distribution is positive (Fig. 1). However, it must be pointed out that in Ref. [8] a different definition of LLD threshold, based on kick, has been used. Moreover, note in Fig. 3 that we could not study the LLD damping beyond a certain intensity. In fact, since the induced voltage of an inductive impedance has a defocusing behaviour on the total potential well, the bunch intensity is limited by the bucket acceptance. In that case, the LLD damping threshold goes to infinity.

Comparison with Simulations

In this subsection, the results of MELODY were compared with macroparticle simulations performed in BLonD. As an example, we used the LHC parameters, listed in Table 1, to simplify the comparison with the results presented in Ref. [2]. In particular, since azimuthal modes are represented by particular frequencies emerging from the incoherent oscillation band, we looked at the spectrum of the mean value of the bunch position. A bunch with 10^6 macroparticles was generated, matched with intensity effects and then tracked for 10^6 turns (in order to have a good frequency resolution of the spectrum and to cover a sufficient number of synchrotron oscillations). Finally, fast Fourier transform of the bunch mean values of the bunch position have been performed to move in the frequency domain.

In Fig. 4, the normalized mode frequencies for different intensities were reported, using both MELODY and BLonD. The comparison was performed considering a constant inductive impedance $Z_{\text{norm}} = 0.07$ Ohm and a cutoff frequency $f_c = 4$ GHz. The computation was repeated for different bunch lengths, in order to cover the most interesting region

Content from this work may be used under the terms of the CC BY 3.0 licence (© 2021). Any distribution of this work must maintain attribution to the author(s), title of the work, publisher, and DOI

ISBN: 978-3-95450-225-7 ISSN: 2673-5571 doi:10.18429/JACoW-HB2021-MOP15

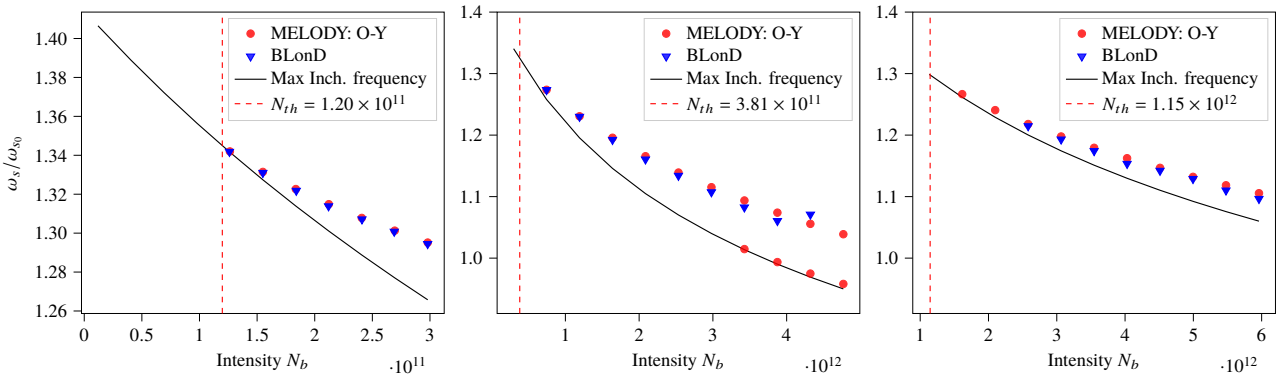

Figure 4: The real part of the normalized mode frequency was found from MELODY, by means of the Oide-Yokoya (O-Y) method [9], and from macroparticle simulations (BLonD) as a function of bunch intensity. The comparison was performed considering a constant inductive impedance with $\mathrm{Im}Z/k = 0.07\ \Omega$ and frequency cutoff $f_c = 4$ GHz. Results for three different bunch lengths, $\phi_{\max} = 1.0$ rad (left), $\phi_{\max} = 1.5$ rad (centre) and $\phi_{max} = 2.0$ rad (right), have been reported to scan different parts of the frequency distribution (Fig.1).

of the synchrotron frequency distribution (Fig.1). A good agreement between macroparticle simulations and semianalytical calculations has been observed, and as expected, coherent dipole modes emerging from the maximum incoherent frequency (black line) can be noticed. Since at the LLD threshold the frequency of the coherent mode equals the maximum incoherent frequency, the modes close to the threshold cannot be discriminated properly from the incoherent band. This explains the missing data for $\phi_{\max} = 2.0$ and in the case of the second emerged mode for $\phi_{\max} = 1.5$.

Table 1: Machine Parameters [10]

Parameter	Values
Circumference	26658.86 m
Main harmonic number, h	35640
Main RF frequency, f_{RF}	400.79 MHz
Beam energy E_0	0.45 TeV
Main RF voltage V_0	6 MV
Normalization factor, Z_{norm}	0.07 Ohm

Beam Response to a Dipole Kick

Observation of the beam response to a kick is a common way to study LLD in either measurements or simulations. In order to simulate a rigid-dipole kick, an instant shift of the bunch position by 1 degree has been introduced at the beginning of the macroparticle simulation. Afterwards, the bunch evolution, up to 5×10^4 turns, has been tracked turn by turn. For simulations, the same parameters in Table 1 and 10^6 macroparticles have been applied. We want to point out that considering a constant inductive impedance with a truncation at f_c, leads to a ringing behaviour of the induced voltage in front and after the bunch. However, since no blow-up was observed, it should not have much impact on the bunch evolution.

Figure 5 shows that, after an initial offset, the bunch position evolution for $\phi_{\max} = 1.0$ (left) and $\phi_{\max} = 1.5$ (centre), with intensities below the LLD thresholds, are quickly damped as predicted. Instead, for larger bunch lengths, in this case for $\phi_{\max} = 2.0$, Figure 5 indicates a counter-intuitive behavior.

We used an analysis based on expansion of the initial perturbation on a basis of van Kampen modes [11, 12] as in Ref. [2]. We observe that at low intensity the damping time can be very long. At higher intensities, the initial damping becomes faster, but the residual oscillation amplitude remains small. The detailed analysis will be presented in an upcoming publication.

CONCLUSION

Landau Damping plays a significant role in beam stabilization. In this work, we focused on the LLD studies for the double harmonic RF system. In particular, special attention has been paid to the 4th harmonic RF system, in BSM. Starting from a constant inductive impedance, with a certain upper cutoff frequency, an analytical expression of the LLD damping for the binomial distribution has been derived. This expression agrees with the semianalytical code MELODY showing a good agreement for both 2nd and 4th harmonic cases. However, we observed a significant loss of accuracy for $f_c/f_{\mathrm{RF}} < 10$ due to the fact that the threshold equation is not applicable for high intensities. Furthermore, MELODY confirmed that the LLD threshold depends inversely on cut-off frequency of the impedance, as observed in the past for single RF systems, and it remains monotonic even for longer bunches length. A comparison between semianalytical calculation and simulation has been set up, showing a very good agreement between the two approaches.

We moved on to evaluate the beam response to a rigid-dipole kick and observing the behaviour of Landau damping under this condition. Particle tracking simulations show that bunches below the threshold are quickly damped as predicted. Exceptions for long bunches have been observed, for which, counterintuitively, bunches with higher intensity

Content from this work may be used under the terms of the CC BY 3.0 licence (© 2021). Any distribution of this work must maintain attribution to the author(s), title of the work, publisher, and DOI

ISBN: 978-3-95450-225-7 ISSN: 2673-5571 doi:10.18429/JACoW-HB2021-MOP15

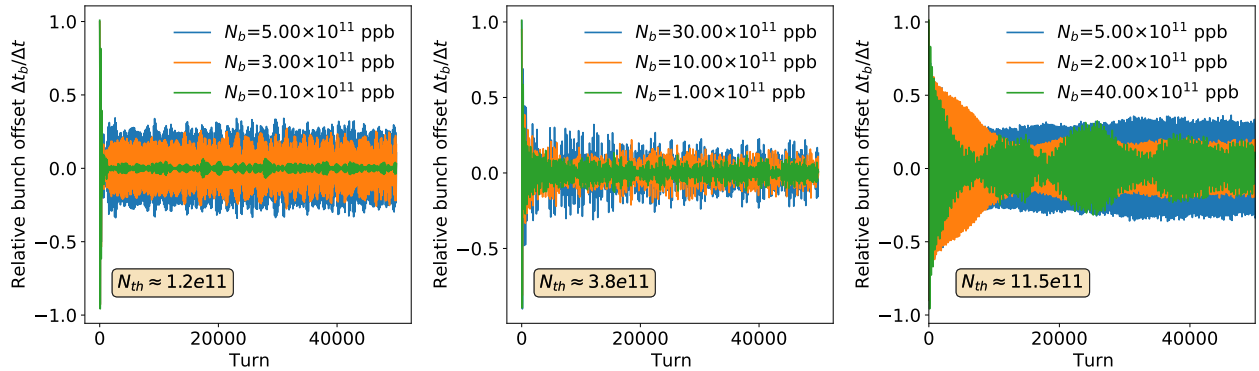

Figure 5: Simulated bunch offset evolution at different intensities, after an initial dipole kick of one degree, with an inductive impedance of $Z_{\text{norm}} = 0.07\ \Omega$ and $f_c = 4$ GHz. Three different bunch lengths, respectively for $\phi_{\max} = 1.0$ rad (left), $\phi_{\max} = 1.5$ rad (centre) and $\phi_{\max} = 2.0$ rad (right) have been considered. For this latter case, 10^7 macroparticles (instead of 10^6) have been chosen to avoid high statistical noise. In all three cases, the respective LLD thresholds in the box have also been reported.

than the LLD threshold, are damped more than those below the threshold. This behavior can be understood by expanding the perturbations on the basis of van Kampen modes.

REFERENCES

[1] L. D. Landau, "On the vibrations of the electronic plasma", *J. Phys. (Moscow)*, vol. 10, p. 25, 1946.

[2] I. Karpov, T. Argyropoulos, and E. Shaposhnikova, "Thresholds for loss of Landau damping in longitudinal plane", *Phys. Rev. Accel. Beams*, vol. 24, p. 011002, 2021. doi:10.1103/PhysRevAccelBeams.24.011002

[3] I. Karpov, "Matrix equations for longitudinal beam dynamics (MELODY) code", https://gitlab.cern.ch/ikarpov/melody/.

[4] CERN beam longitudinal dynamics code BLonD, http://blond.web.cern.ch/.

[5] A. N. Lebedev, "Coherent synchrotron oscillations in the presence of a space charge", *Soviet Atomic Energy*, vol. 25, p. 851, 1968. doi:10.1007/BF01121037

[6] E. Shaposhnikova, "Bunched beam transfer matrices in single and double rf systems", Technical Report No. CERN-SL-94-19-RF, CERN, Geneva, Switzerland, 1994.

[7] P. Bramham, S. Hansen, A. Hofmann and P. Peschardt, "Active Landau Cavity on the 4th Harmonic of the RF Frequency", ISR Performance Report, CERN, Geneva, Switzerland, 1977.

[8] A. Theodoros, "Longitudinal beam instabilities in a double RF system", Ph.D. Thesis, Natl. Tech. U., Athens, 2015.

[9] K. Oide and K. Yokoya, "Longitudinal single bunch instability in electron storage rings", Technical Report, No. KEK-Preprint-90, KEK, Tsukuba, Japan, 1990.

[10] O. Brüning *et al.*,LHC Design Report Vol.1: The LHC main ring, CERN, Geneva, Switzerland, Tech. Rep. CERN-2004-003-V-1, Jun.2004.

[11] N. G. van Kampen, "On the theory of stationary waves in plasmas", *Physica (Utrecht)*, vol. 21, p. 949, 1955. doi:10.1016/S0031-8914(55)93068-8

[12] N. G. van Kampen, "The dispersion equation for plasma waves", *Physica (Utrecht)*, vol. 23, p. 641, 1957. doi:10.1016/S0031-8914(57)93718-7

Content from this work may be used under the terms of the CC BY 3.0 licence (© 2021). Any distribution of this work must maintain attribution to the author(s), title of the work, publisher, and DOI